ASTRONOMY & ASTROPHYSICS
SUPPLEMENT SERIES

Astron. Astrophys. Suppl. Ser. **129,** 161-172 (1998)

Atomic data from the IRON Project

XXVIII. Electron excitation of the $^2P^\circ_{3/2} \rightarrow {}^2P^\circ_{1/2}$ fine structure transition in fluorine-like ions at higher temperatures

K.A. Berrington[1], **H.E. Saraph**[2], **and J.A. Tully**[3]
[1] Department of Applied Mathematics & Theoretical Physics, The Queen's University of Belfast, Belfast BT7 1NN, UK
[2] Department of Physics & Astronomy, University College London, Gower Street, London WC1E 6BT, UK
[3] Département Giovanni Domenico Cassini, Observatoire de la Côte d'Azur, BP. 4229, 06304 Nice Cedex 4, France

Received July 17; accepted September 12, 1997

Abstract. The collision strength $\Omega(^2P^o_{3/2}, {}^2P^o_{1/2})$ for the fine structure transition within the ground term of 17 fluorine-like ions from Mg IV to Ni XX is calculated using the R-matrix method. We include target terms with $n = 3$ in order to take account of the resonance structure in Ω at energies above $2s2p^6\,{}^2S$. These resonances are delineated using a fine mesh of several thousand energy points to scan the region between the first and 27th excited terms. Results from an earlier calculation (IRON Project Paper IV) are used to cover the region below $2s2p^6\,{}^2S$. We make use of the fact that Ω tends to the Born limit as the collision energy $E \rightarrow \infty$. The effective collision strength Υ is tabulated as a function of $\log T_s$, where $T_s = T/(Z-8)^2$ is a Z-scaled temperature. We compare results for Si^{+5}, Fe^{+17} and Ni^{+19} with those obtained by Mohan and coworkers. An explanation is given for the large discrepancy in the case of $\Upsilon(Si^{+5})$.

Key words: atomic data — atomic processes

1. Introduction

The present calculation forms part of the IRON Project, an international joint undertaking whose aims are spelt out by Hummer et al. (1993). This, being the first paper of the project, is henceforth referred to as IP I. In IP IV, Saraph & Tully (1994) give thermally averaged collision strengths for the ground term fine structure transition in fluorine like ions from Ne II to Fe XVIII. These authors used a simple target consisting of the two terms $2s^22p^5\,{}^2P^o$ and $2s2p^6\,{}^2S$. They included in their model a non spectroscopic orbital $\bar{3}d$ which greatly improved the theoretical term energies. In this way it was possible to obtain reliable rate coefficients at relatively low temperatures, such as those associated with photoionized nebular clouds for example.

Here we use an extended target representation of 28 terms. At energies between $2s2p^6\,{}^2S$ and the 28th term the resulting collision strengths all contain resonance structures caused by quasi-bound states that converge onto these terms. We delineate these resonances by calculating Ω at several thousand energies above $2s2p^6\,{}^2S$. Our results for Ω at these higher energies are combined with those from IP IV and used to obtain thermally averaged collision strengths $\Upsilon(2p^5\,{}^2P^o_{3/2}, 2p^5\,{}^2P^o_{1/2})$ which we estimate should be reliable at the higher temperatures typical of coronal ionization equilibrium conditions. We include the ions Co^{+18} and Ni^{+19} which were not dealt with in IP IV. For these we carried out a 2-term calculation, as in IP IV, in order to cover the energy range between the ground $(2p^5\,{}^2P^o)$ and first excited $(2s2p^6\,{}^2S)$ terms. The observed energy of this interval is estimated to be 9.944962 Ry for $Z = 27$ and 10.51617 Ry for $Z = 28$.

We make use of the rydberg (Ry) energy unit. For this we adopt the value 1 Ry = 109737.32 cm^{-1} which corresponds to a wavelength of 911.267 Å. All of the IRON Project papers that have been published to date are given in the references section. Details of these and of papers that are in press are also available on the Internet at http://www.am.qub.ac.uk.

2. The calculation

The basic atomic theory employed in the IRON Project, including methodology and computer codes, is described in IP I. Collision strengths for fine structure transitions are calculated from collision data obtained in *LS* coupling by using an algebraic transformation to intermediate coupling, as described in Sect. 2.6 of IP I (see also Saraph 1978). This method neglects the fine structure splitting of the target terms.

Table 1. Configurations that give rise to the 28 lowest terms of fluorine-like ions. Parent terms are shown and each configuration includes $1s^2$. Correlation configurations used in the target are also listed

Label	Configuration	Label	Configuration
1	$2s^2 2p^5$	11	$2s^2 2p^4(^1S)3d$
2	$2s2p^6$	12	$2s2p^5(^3P^o)3s$
3	$2s^2 2p^4(^3P)3s$	13	$2s2p^5(^3P^o)3p$
4	$2s^2 2p^4(^3P)3p$	14	$2s2p^5(^3P^o)3d$
5	$2s^2 2p^4(^3P)3d$	15	$2s2p^5(^1P^o)3s$
6	$2s^2 2p^4(^1D)3s$	16	$2s2p^5(^1P^o)3p$
7	$2s^2 2p^4(^1D)3p$	17	$2s2p^5(^1P^o)3d$
8	$2s^2 2p^4(^1D)3d$	18	$2p^6(^1S)3s$
9	$2s^2 2p^4(^1S)3s$	19	$2p^6(^1S)3p$
10	$2s^2 2p^4(^1S)3p$	20	$2p^6(^1S)3d$

Correlation configurations

$2p^5 3l3l'$
$2s2p^4 3l3l'$
$2s^2 2p^3 3l3l'$
$2s^2 2p^2 3s3p3d$
$2s2p^3 3s3p3d$
$2p^4 3s3p3d$

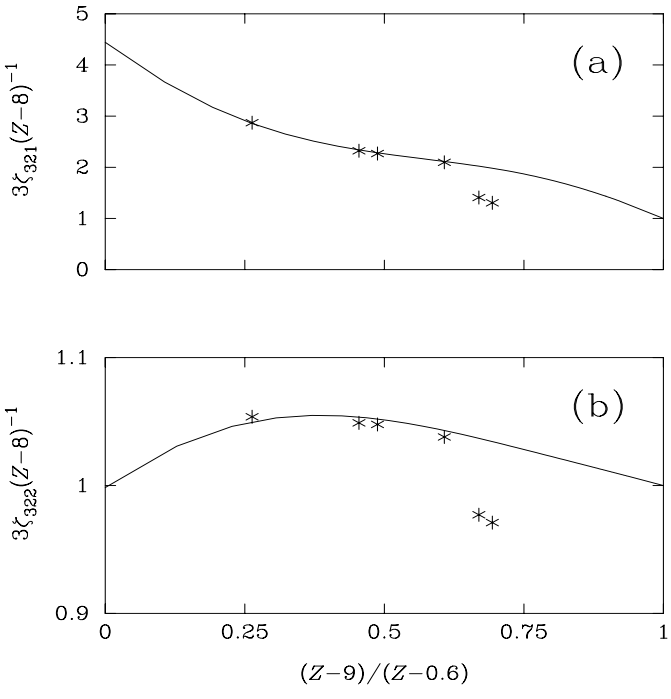

Fig. 1. Full line curves are cubic spline fits to data in Table 2 with rms errors **a)** 0.5% and **b)** 0.01%. The starred points $*$ correspond to results from Mohan & Hibbert (1991)

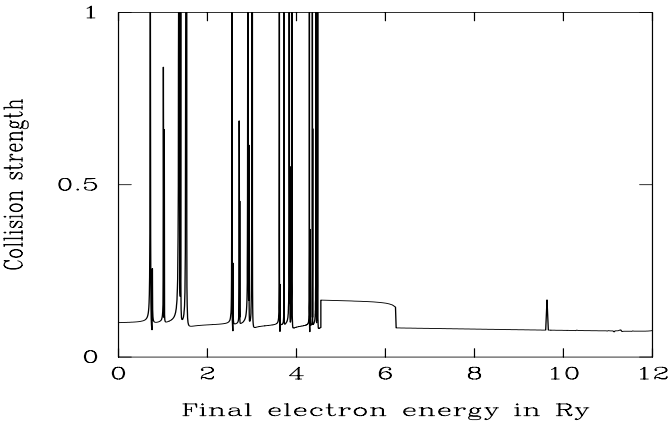

Fig. 2. Ca^{+11}: $\Omega(2p^5\,{}^2P^o_{3/2},\ 2p^5\,{}^2P^o_{1/2})$

2.1. The target

Here we take account of the autoionization processes that can affect the cross section of the fine structure transition in the $^2P^o$ ground term at collision energies up to that required to excite the 28th target term $2s^2 2p^4(^1S)3d\,^2D$. Thus the energy range covered by the present paper is twice that of IP IV for the lighter ions and ten times that for the iron group ions. The dominant configuration in terms 3 to 28 is $2s^2 2p^4\,3l$, where $3l$ is a spectroscopic orbital with $0 \le l \le 2$. We take the radial orbitals $P_{1s}\,, P_{2s}\,, P_{2p}$ from Clementi & Roetti (1974) and calculate $P_{3s}\,, P_{3p}\,, P_{3d}$ using Hibbert's (1975) program CIV3. The parameterised form of $P_{3l}(r)$ is the one used by Clementi & Roetti (1974), namely

$$P_{3l}(r)/r = \sum_{p=1}^{k} C_{3lp} R_{3lp}(r)\,, \qquad (1)$$

where

$$R_{3lp}(r) = \Big[\frac{(2\zeta_{3lp})^{2n_{3lp}+1}}{(2n_{3lp})!}\Big]^{1/2} r^{n_{3lp}-1} \exp(-\zeta_{3lp} r). \qquad (2)$$

Our choice for the integers $(k,\, n_{3lp})$ in Eqs. (1) and (2) is $(3,\, p)$ for $l = 0$, $(2,\, 1+p)$ for $l = 1$ and $(2,\, 3)$ for $l = 2$. The values we give in Table 2 for C_{3lp} and ζ_{3lp} were obtained following the procedure adopted by Mohan & Hibbert (1991). That is to say, the parameters of each P_{3l} were varied in order to minimise the energies of selected terms: $2p^4\,(^1D)3s\ ^2D$ for 3s; $2p^4\,(^3P)3p\ ^2D^o$ for 3p; $2p^4\,(^3P)3d\ ^2F$ for 3d. Having obtained satisfactory $n = 3$ orbitals for singly ionized neon we then used the Ne^+ parameters as initial trial values for Na^{+2}. The optimised parameters obtained in this way for Na^{+2} were then used as trial values for Mg^{+3} and so on along the sequence as far as Ni^{+19}. In all cases we used the minimization code MODDAV by setting the CIV3 parameter IDAVID = 0.

Mohan & Hibbert (1991) have obtained spectroscopic $n = 3$ orbitals with CIV3 for six of the ions dealt with here. Our 3s, 3p, 3d orbitals are in satisfactory agreement with

Table 2. Fluorine sequence: radial orbital parameters. For each Z, nlp the upper (lower) number is the value of ζ_{nlp} (C_{nlp})

Z	$nlp = 301$	$nlp = 302$	$nlp = 303$	$nlp = 311$	$nlp = 312$	$nlp = 321$	$nlp = 322$
10	8.095246	3.266739	1.163410	3.530236	0.923711	2.462823	0.687194
	0.099730	−0.356887	1.036262	0.260780	−1.000634	0.031488	0.991278
11	8.919863	3.567821	1.515644	4.009371	1.256699	3.136974	1.046041
	0.120510	−0.451041	1.074791	0.320611	−1.012196	0.049018	0.981038
12	9.690180	3.883820	1.850745	4.480893	1.580585	3.791358	1.403897
	0.135930	−0.525640	1.115100	0.367303	−1.025859	0.058978	0.972880
13	10.42993	4.205650	2.183463	4.945376	1.900644	4.427342	1.758242
	0.148996	−0.591966	1.156396	0.403524	−1.040423	0.063832	0.967407
14	11.14813	4.530462	2.515404	5.404015	2.218909	5.050042	2.109039
	0.160455	−0.652979	1.197579	0.434109	−1.054911	0.065677	0.964041
15	11.85268	4.854268	2.847533	5.857134	2.536399	5.662291	2.456780
	0.170602	−0.708773	1.238524	0.465932	−1.068586	0.065850	0.962103
16	12.54460	5.177604	3.179915	6.305809	2.853645	6.267704	2.802139
	0.179721	−0.761515	1.278762	0.483432	−1.082715	0.065052	0.961141
17	13.22786	5.499258	3.512871	6.750348	3.170891	6.867074	3.145558
	0.172211	−0.756212	1.310172	0.503925	−1.095817	0.063741	0.960803
18	13.90064	5.820202	3.846325	7.191539	3.488298	7.462762	3.487506
	0.195803	−0.859568	1.357124	0.522634	−1.108325	0.062132	0.960898
19	14.56788	6.137855	4.180618	7.629962	3.805878	8.055196	3.828262
	0.202908	−0.905610	1.395478	0.539956	−1.120237	0.060383	0.961273
20	15.22800	6.453572	4.515461	8.065201	4.123840	8.644899	4.167991
	0.209521	−1.950061	1.433188	0.555645	−1.131662	0.058593	0.961825
21	15.88471	6.761167	4.852479	8.497378	4.442167	9.232155	4.506887
	0.215631	−0.994645	1.472043	0.569899	−1.142626	0.056812	0.962487
22	16.53345	7.069813	5.189106	8.927572	4.760788	9.817833	4.845138
	0.221396	−1.037152	1.509494	0.583375	−1.153084	0.055063	0.963224
23	17.17390	7.375341	5.526314	9.356097	5.079613	10.40225	5.182819
	0.226692	−1.078626	1.546702	0.596156	−1.163055	0.053365	0.964003
24	17.81315	7.677423	5.864517	9.782190	5.398982	10.98535	5.520072
	0.231902	−1.120129	1.584103	0.608036	−1.172668	0.051732	0.964801
25	18.44708	7.979157	6.202479	10.20699	5.718553	11.56755	5.856933
	0.236923	−1.160460	1.620604	0.619405	−1.181851	0.050166	0.965604
26	19.08486	8.266246	6.544050	10.62908	6.038546	12.14856	6.193407
	0.249244	−1.252445	1.699552	0.629756	−1.190742	0.048676	0.966397
27	19.70004	8.571291	6.880852	11.05077	6.358677	12.73139	6.526987
	0.246277	−1.240695	1.694465	0.639960	−1.199214	0.047153	0.967271
28	20.32927	8.847834	7.223726	11.47005	6.679255	13.31948	6.864242
	0.250387	−1.284260	1.736172	0.649441	−1.207438	0.046126	0.967818

theirs, except for 3d ($Z = 26, 28$). We have no explanation why Mohan & Hibbert's 3d parameters for these two ions deviate from the smooth behaviour exhibited lower down the sequence. Figures 1a and 1b, which make use of the isoelectronic fitting procedure proposed by Burgess et al. (1997a), illustrate this point.

Blackford & Hibbert (1994) have also studied fluorine-like ions using CIV3, but their $n = 3$ orbitals are non-spectroscopic.

Table 1 lists the configurations that we include for the construction of the target terms. The first 28 terms that can be constructed from these configurations were included in the close-coupling expansion for the scattering calculation. They have dominant configurations labelled 1 to 11 and their calculated energies are given in Table 3, where a scaling factor $(Z-9)^{-2}$ is applied for convenience.

2.2. Collision strength $\Omega(^2\mathrm{P}^{\mathrm{o}}_{3/2}\,,\,^2\mathrm{P}^{\mathrm{o}}_{1/2})$

The results for Ω from the extended target join on fairly smoothly at the $2s2p^6\ ^2S$ threshold to those from the 2-term calculation (IP IV). This is because, as predicted in IP IV, resonances caused by the 26 higher terms start to enhance the collision strength at energies well above $2s2p^6\ ^2S$ for ions with $Z \geq 12$. The 26 terms arising from configurations $2s^22p^43l$ with $0 \leq l \leq 2$, lie energetically

Table 3. Theoretical term energies for the fluorine sequence in $(Z-9)^2$ Ry. Label refers to configurations given in Table 1

Label	Term	$Z=12$	$Z=13$	$Z=14$	$Z=15$	$Z=16$	$Z=17$
11	^{2}D	0.76509	0.57471	0.47113	0.40655	0.36263	0.33091
8	^{2}D	0.73354	0.55500	0.45745	0.39642	0.35476	0.32460
8	^{2}P	0.73145	0.55377	0.45670	0.39593	0.35444	0.32437
8	^{2}F	0.73326	0.55411	0.45618	0.39493	0.35317	0.32295
8	^{2}S	0.73162	0.55297	0.45534	0.39427	0.35263	0.32250
8	^{2}G	0.72757	0.54955	0.45239	0.39168	0.35033	0.32043
5	^{2}D	0.70069	0.53418	0.44236	0.38454	0.34492	0.31614
5	^{2}P	0.70167	0.53432	0.44211	0.38410	0.34440	0.31559
5	^{2}F	0.69690	0.53081	0.43948	0.38209	0.34283	0.31435
5	^{4}P	0.69673	0.53045	0.43905	0.38165	0.34239	0.31392
5	^{4}F	0.69430	0.52849	0.43741	0.38024	0.34116	0.31283
5	^{4}D	0.68862	0.52390	0.43357	0.37694	0.33827	0.31026
10	^{2}P^o	0.69524	0.52486	0.43264	0.37532	0.33641	0.30835
7	^{2}P^o	0.68138	0.51666	0.42700	0.37109	0.33304	0.30557
7	^{2}D^o	0.66177	0.50287	0.41651	0.36271	0.32611	0.29968
7	^{2}F^o	0.65414	0.49747	0.41238	0.35936	0.32332	0.29729
4	^{4}S^o	0.62893	0.48202	0.40165	0.35133	0.31698	0.29210
4	^{2}S^o	0.62893	0.48202	0.40165	0.35133	0.31698	0.29210
4	^{2}D^o	0.62533	0.47946	0.39968	0.34974	0.31565	0.29095
4	^{2}P^o	0.62949	0.48141	0.40067	0.35025	0.31590	0.29105
4	^{4}D^o	0.61927	0.47520	0.39643	0.34712	0.31347	0.28909
9	^{2}S	0.63268	0.48077	0.39878	0.34793	0.31347	0.28865
4	^{4}P^o	0.61116	0.46944	0.39200	0.34354	0.31048	0.28652
6	^{2}D	0.59817	0.45835	0.38264	0.33527	0.30317	0.27999
3	^{2}P	0.57145	0.44153	0.37057	0.32618	0.29589	0.27396
3	^{4}P	0.55856	0.43289	0.36418	0.32116	0.29179	0.27051
2	^{2}S	0.32916	0.21074	0.15127	0.11644	0.09361	0.07830
1	^{2}P^o	0.00000	0.00000	0.00000	0.00000	0.00000	0.00000

close together and this means that the associated resonances form a dense "forest" of spikes covering a broad energy region. The widths of these spikes and the windows between them are very narrow compared to that of the electron velocity distribution function. Since it is our aim to calculate effective collision strengths it is not necessary, at these high excitation energies, to identify individual resonances, or to obtain their positions to high accuracy. Instead we obtain the collision strength to sufficient detail so that the average is correct. In any case, measurements that might allow one to replace calculated term energies by experimental values are incomplete for the higher terms and therefore we could not correct the target term energies empirically as was done in IP IV. At low temperatures, it will be recalled, the width of the velocity distribution function and those of the resonances are comparable and therefore the correct positioning of the low energy resonances due to the term $2s2p^6\ ^2S$ dramatically affects the low temperature effective collision strength of several ions.

We illustrate the complicated energy dependence of our collision strengths by plotting $\Omega(Ca^{+11})$ in Figs. 2 to 10 as a function of E_f from threshold (i.e. $E_f = 0$) to a value just above that necessary to excite the 28th term. The collision strength is obtained using different steplengths in four distinct energy bands. From threshold up to $2s2p^6\ ^2S$ we use the collision strength obtained in IP IV. Then at energies between the second and third terms, i.e. between $2s2p^6\ ^2S$ and $2s^22p^43s\ ^4P$, the collision strength is calculated using an energy mesh based on equal steps in effective quantum number ν, see IP IV. This mesh is ideal for delineating the resonance structure in this interval and about 3600 mesh points are used for each ion. Partial wave contributions are summed up to $J = 7$. The energy range from just below the 3rd term and up to the 28th term was scanned at constant steps in energy δE: between the 3rd and 17th terms $\delta E = x\ 10^{-5}(Z-9)^2$ and between the 17th and 28th terms $\delta E = x\ 10^{-4}(Z-9)^2$, where x varies between $x = 3$ for the lighter ions and $x = 1$ for the heavier ones. We found that the resonances were in all cases less prominent at energies between terms 17 and 28 which is why we could use a coarser mesh. From the 3rd threshold onwards, i.e. for $E_f > |\epsilon_1 - \epsilon_3|$, partial waves were summed up to $J = 10$. At energies above

Table 3. continued

Label	Term	$Z=18$	$Z=19$	$Z=20$	$Z=21$	$Z=22$	$Z=23$
11	^{2}D	0.30696	0.28826	0.27327	0.26099	0.25075	0.24208
8	^{2}D	0.30176	0.28388	0.26951	0.25772	0.24787	0.23952
8	^{2}P	0.30160	0.28376	0.26943	0.25766	0.24782	0.23949
8	^{2}F	0.30010	0.28225	0.26791	0.25616	0.24636	0.23805
8	^{2}S	0.29972	0.28191	0.26761	0.25589	0.24611	0.23783
8	^{2}G	0.29784	0.28019	0.26604	0.25444	0.24479	0.23656
5	^{2}D	0.29432	0.27723	0.26348	0.25220	0.24278	0.23479
5	^{2}P	0.29377	0.27669	0.26297	0.25171	0.24231	0.23434
5	^{2}F	0.29276	0.27586	0.26227	0.25112	0.24180	0.23390
5	^{4}P	0.29236	0.27547	0.26191	0.25077	0.24147	0.23359
5	^{4}F	0.29137	0.27458	0.26109	0.25002	0.24077	0.23293
5	^{4}D	0.28907	0.27249	0.25918	0.24826	0.23914	0.23142
10	^{2}P^o	0.28720	0.27070	0.25746	0.24662	0.23758	0.22994
7	^{2}P^o	0.28484	0.26865	0.25566	0.24501	0.23613	0.22862
7	^{2}D^o	0.27972	0.26412	0.25161	0.24136	0.23281	0.22556
7	^{2}F^o	0.27762	0.26226	0.24994	0.23984	0.23142	0.22428
4	^{4}S^o	0.27326	0.25851	0.24667	0.23695	0.22882	0.22194
4	^{2}S^o	0.27326	0.25851	0.24667	0.23695	0.22882	0.22194
4	^{2}D^o	0.27226	0.25762	0.24586	0.23622	0.22816	0.22132
4	^{2}P^o	0.27226	0.25756	0.24576	0.23609	0.22802	0.22117
4	^{4}D^o	0.27063	0.25618	0.24457	0.23504	0.22708	0.22033
9	^{2}S	0.26993	0.25534	0.24365	0.23407	0.22610	0.21935
4	^{4}P^o	0.26838	0.25418	0.24277	0.23342	0.22560	0.21896
6	^{2}D	0.26248	0.24881	0.23785	0.22886	0.22136	0.21501
3	^{2}P	0.25735	0.24436	0.23392	0.22536	0.21820	0.21214
3	^{4}P	0.25438	0.24176	0.23161	0.22328	0.21632	0.21041
2	^{2}S	0.06693	0.05831	0.05157	0.04617	0.04176	0.03810
1	^{2}P^o	0.00000	0.00000	0.00000	0.00000	0.00000	0.00000

all 28 thresholds collision strengths were obtained on a very coarse mesh but particular attention was paid to the convergence with respect to angular momentum J. The contributions from the two highest partial waves ($J = 9$ and 10) were taken to fit a geometric series and thus used to estimate a top-up to the collision strengths. Near the energy of the 28th term this top-up amounted to about 2% of the total and it gradually increased to 10% at around four times that energy. Tabulation was stopped at this point and, for the purpose of calculating effective collision strengths, the high energy results were then spline fitted including a value at $E = \infty$ obtained in the Born approximation (Burgess et al. 1997b). These limiting Born values are given in Table 4.

2.3. Effective collision strength $\Upsilon(^2\mathrm{P}^\mathrm{o}_{3/2}\,,\,^2\mathrm{P}^\mathrm{o}_{1/2})$

Seaton (1953) defines the thermally averaged, or effective, collision strength Υ_{if} for a transition $i \rightarrow f$ to be the integral

$$\Upsilon_{if}(T) = \int_0^\infty \Omega_{if}(E_f)\,\exp\bigl(-E_f/kT\bigr)\mathrm{d}\bigl(E_f/kT\bigr). \qquad (3)$$

Since our calculation is in LS coupling it ignores the fine structure energy splitting. This means that the incident and final collision energies E_i, E_f are identical. In Table 5 we tabulate $\Upsilon(^2\mathrm{P}^\mathrm{o}_{3/2}\,,\,^2\mathrm{P}^\mathrm{o}_{1/2})$ as a function of $\log T_\mathrm{s}$, where $T_\mathrm{s} = T/(Z-8)^2$ is a scaled temperature that is convenient to use for the fluorine isoelectronic sequence. The present results agree with those in IP IV except at the highest temperature for each ion considered in IP IV where the earlier results are usually a few percent lower.

It is important to understand the validity of approximations made in the current scattering calculations. First, one establishes the range of temperatures over which data are required. Next, one determines the range of energies for which accurate collision data need to be calculated. Table 6 shows the relative contributions to the total effective collision strength from the four different energy bands defined in Sect. 2.2 as a function of temperature. As discussed in IP IV, the isolated resonances in the first band must be delineated to the best possible accuracy because the velocity distribution function emphasizes these structures in a very selective way. Resonances in the second band are narrower relative to the width of the distribution

Table 3. continued

Label	Term	$Z = 24$	$Z = 25$	$Z = 26$	$Z = 27$	$Z = 28$
11	^{2}D	0.23465	0.22822	0.22261	0.21762	0.21321
8	^{2}D	0.23235	0.22613	0.22071	0.21587	0.21159
8	^{2}P	0.23233	0.22612	0.22071	0.21587	0.21160
8	^{2}F	0.23093	0.22476	0.21939	0.21460	0.21036
8	^{2}S	0.23073	0.22457	0.21920	0.21443	0.21020
8	^{2}G	0.22954	0.22345	0.21815	0.21343	0.20926
5	^{2}D	0.22793	0.22199	0.21680	0.21218	0.20810
5	^{2}P	0.22750	0.22158	0.21641	0.21181	0.20774
5	^{2}F	0.22712	0.22124	0.21612	0.21155	0.20750
5	^{4}P	0.22682	0.22095	0.21584	0.21128	0.20725
5	^{4}F	0.22621	0.22038	0.21530	0.21077	0.20677
5	^{4}D	0.22480	0.21905	0.21404	0.20959	0.20564
10	^{2}P^o	0.22338	0.21771	0.21274	0.20836	0.20447
7	^{2}P^o	0.22217	0.21659	0.21170	0.20739	0.20356
7	^{2}D^o	0.21935	0.21397	0.20926	0.20510	0.20141
7	^{2}F^o	0.21817	0.21286	0.20823	0.20413	0.20049
4	^{4}S^o	0.21603	0.21090	0.20641	0.20244	0.19892
4	^{2}S^o	0.21603	0.21090	0.20641	0.20244	0.19892
4	^{2}D^o	0.21546	0.21037	0.20591	0.20198	0.19848
4	^{2}P^o	0.21530	0.21021	0.20576	0.20182	0.19832
4	^{4}D^o	0.21454	0.20952	0.20512	0.20123	0.19777
9	^{2}S	0.21356	0.20855	0.20416	0.20030	0.19686
4	^{4}P^o	0.21327	0.20833	0.20401	0.20019	0.19679
6	^{2}D	0.20957	0.20485	0.20071	0.19707	0.19383
3	^{2}P	0.20693	0.20241	0.19845	0.19496	0.19185
3	^{4}P	0.20534	0.20094	0.19709	0.19368	0.19066
2	^{2}S	0.03500	0.03236	0.03008	0.02809	0.02634
1	^{2}P^o	0.00000	0.00000	0.00000	0.00000	0.00000

function. Consequently the exact position is no longer so crucial but good delineation is still very important. This is ensured by the use of a steplength $\delta\nu$ that is a function of effective quantum number ν calculated relative to the third target term $2s^2 2p^4 3s\,^4P$. The step size therefore decreases as $(\Delta\epsilon)^{3/2}$, where $\Delta\epsilon$ is the energy separation from the third target term. The third band would pose considerable computational problems if one wanted to cover it using a fixed steplength $\delta\nu$ because of the many overlapping resonances from different channels. However, their mean contribution to the total effective collision strength can be obtained by using energy sampling at a moderately small steplength δE (see Saraph & Storey 1996). The last (i.e. fourth) band contributes very little although it is infinite in size. In order to include all collision channels here one would have to increase the close coupling expansion further and further, including also continuum states beyond the ionization threshold. Such calculations are very demanding on computer time (see Pelan & Berrington 1997), but fortunately they are not necessary for the present purposes. The ions considered in this paper have maximum coronal abundances at temperatures between 10^5 K and 10^7 K, and the present calculations are accurate for these temperatures because the higher energy bands, for which this calculation is rather crude, contribute relatively little.

We note that the present high temperature results tend to the Born limit where $\Upsilon(T \to \infty) = \Omega(E \to \infty)$. Values of the limit for neutral fluorine and all ions in the sequence as far as Ni^{+19} are given in Table 4.

3. Comparison with other work

Numerous papers for the transition dealt with here have appeared over the past 10 years or so. These have all been based on essentially the same R-matrix suite of programs as the one we use, but with different target wavefunctions. Obviously it is important to compare some of this earlier work with ours, especially in those cases where there exist significant differences between the Υ results. Note that the comparisons we make concern calculations in which the target wavefunctions have more than two terms.

The three ions we have selected for comparison, namely those corresponding to $Z = 14$, 26 and 28, have been studied by Mohan and collaborators: Si^{+5} (Mohan & Le Dourneuf 1990), Fe^{+17} (Mohan et al. 1987), Ni^{+19} (Mohan

Table 4. (a) High energy limiting values of $10 \times \Omega$ obtained by spline fitting the Born results of Burgess et al. (1997b) in the manner proposed by Burgess et al. (1997a). (b) Logarithm of the temperature of maximum coronal abundance obtained by spline fitting the data given in Arnaud & Rothenflug (1985), see Burgess et al. (1997a). (c) The fine structure transition energy $\epsilon_{\rm fs}$ in Ry from Edlén's (1969) fit to observed intervals

Ion	(a)	(b)	(c)
F	4.040	3.609	0.00368
Ne^{+}	2.678	4.600	0.00711
Na^{+2}	1.922	4.999	0.01245
Mg^{+3}	1.452	5.205	0.02031
Al^{+4}	1.137	5.375	0.03138
Si^{+5}	0.9156	5.543	0.04642
P^{+6}	0.7540	5.706	0.06628
S^{+7}	0.6317	5.857	0.09191
Cl^{+8}	0.5373	5.991	0.12432
Ar^{+9}	0.4628	6.111	0.16462
K^{+10}	0.4027	6.217	0.21402
Ca^{+11}	0.3537	6.312	0.27379
Sc^{+12}	0.3133	6.396	0.34532
Ti^{+13}	0.2793	6.471	0.43008
V^{+14}	0.2508	6.538	0.52963
Cr^{+15}	0.2262	6.599	0.64562
Mn^{+16}	0.2052	6.654	0.77982
Fe^{+17}	0.1870	6.704	0.93408
Co^{+18}	0.1711	6.750	1.11036
Ni^{+19}	0.1572	6.792	1.31071

et al. 1990). Each of these raises questions which we now comment on.

3.1. Si VI

Mohan & Le Dourneuf (1990) tabulate the effective collision strength $\Upsilon(^2\mathrm{P}^{\rm o}_{3/2}\,,\,^2\mathrm{P}^{\rm o}_{1/2})$ for Si VI as a function of temperature. They calculated Υ using the collision strength they had obtained earlier by means of a 16 state close-coupling expansion in LS coupling. As can be seen in Fig. 11, where we plot Υ as a function of $\log T$, their tabulated results rise dramatically with temperature when this exceeds about $2\ 10^5$ K. Burgess et al. (1991) were able to make a reliable spline fit to Mohan & Le Dourneuf's data using the program OMEUPS (see Burgess & Tully 1992), the r.m.s. error of the fit being 2.2%. In order to get a fit to this accuracy Burgess et al. (1991) omitted the lowest two temperature points given in the table. Mohan (private communication) had previously informed one of us (JAT) that the published value at the lowest temperature, i.e. $\Upsilon = 0.4216$, was unreliable. However he gave no explanation why this was so.

Saraph & Tully (1994) state that at higher temperatures (not energies, as printed incorrectly in their paper) the results of Mohan & Le Dourneuf (1990) indicate a steep rise in the effective collision strength that is due to resonances converging on higher target states (i.e. on terms above $2s2p^6\ ^2S$). The present investigation shows, however, that the reason for the increase manifested by the starred data points in Fig. 11 is principally due to the fact that Mohan & Le Dourneuf (1990) used the trapezoidal rule to carry out the integration over energy. Since there is a big gap in their tabulation of Ω between about 10 Ry and 48 Ry, this numerical method should not have been used; see Burgess et al (1997b) for a detailed explanation.

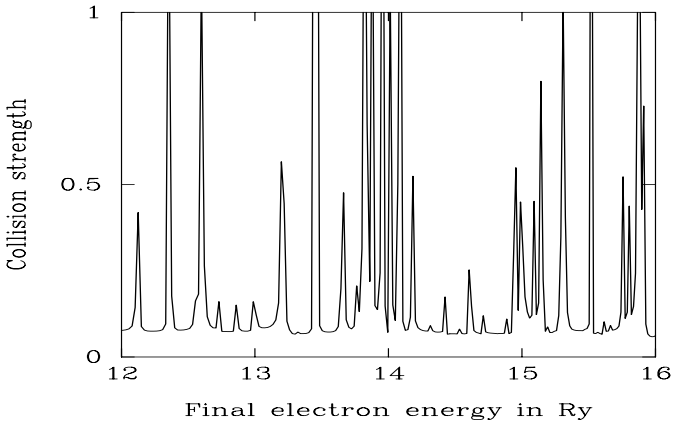

Fig. 3. Ca^{+11}: $\Omega(2p^5\ ^2P^{\rm o}_{3/2}\,,\ 2p^5\ ^2P^{\rm o}_{1/2})$

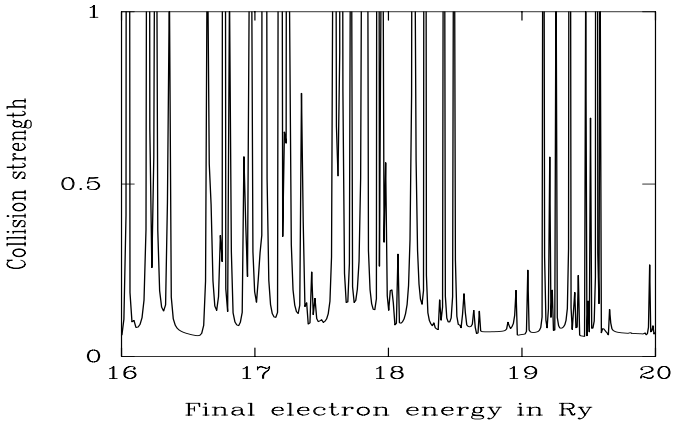

Fig. 4. Ca^{+11}: $\Omega(2p^5\ ^2P^{\rm o}_{3/2}\,,\ 2p^5\ ^2P^{\rm o}_{1/2})$

The gap is apparent in Fig. 12a where we plot $\Omega(Si^{+5})$ as a function of energy: the collision strength is taken from the atomic databank at The Queen's University of Belfast (QUB). The gap is spanned in the figure by a dashed straight line. The resonances above 48 Ry in Fig. 12a, i.e. *above* the highest target term included by Mohan & Le Dourneuf, are clearly responsible for the peak in Υ

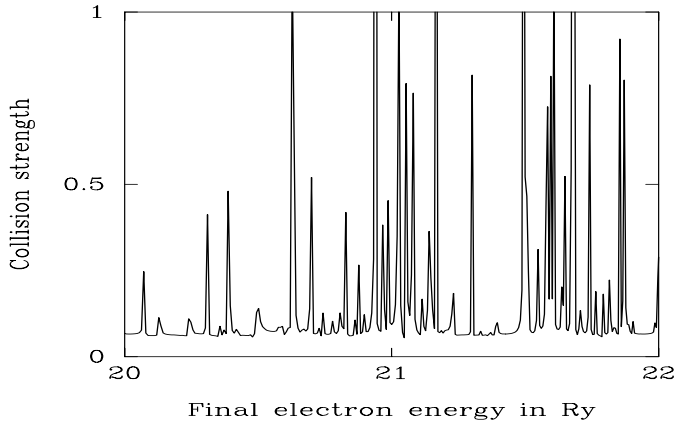

Fig. 5. Ca^{+11}: $\Omega(2p^5\ ^2P^o_{3/2},\ 2p^5\ ^2P^o_{1/2})$

near $\log T = 6$ seen in Fig. 11 (curves a and b). The origin and physical significance, if any, of these resonances have not been explained by Mohan and Le Dourneuf. Fig. 12b shows that, as is to be expected, Ω from the IRON Project has no structure in the region beyond about 12 Ry. Consequently the resulting curve c in Fig. 11 does not have a peak in the region of $\log T = 6$.

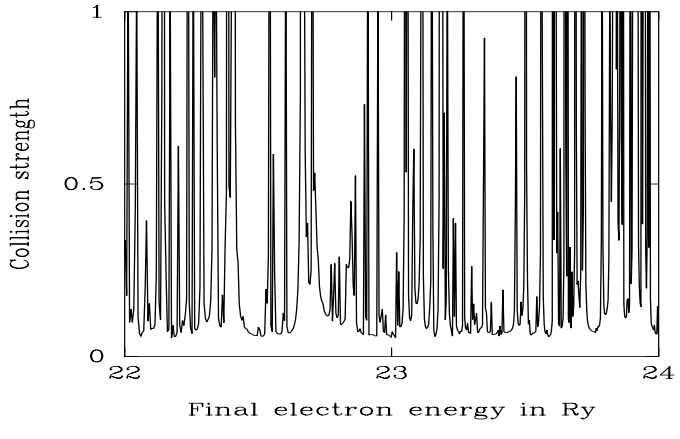

Fig. 6. Ca^{+11}: $\Omega(2p^5\ ^2P^o_{3/2},\ 2p^5\ ^2P^o_{1/2})$

3.2. Fe XVIII

Saraph & Tully (1994) state that the effective collision strength given by Mohan et al. (1987) rises steeply at higher energies. This is wrong on two counts. Firstly, since the effective collision strength is a function of T they should have said "at higher temperatures" and not "at higher energies". Secondly, the effective collision strength that Mohan et al. (1987) tabulate does not vary enormously with temperature. As can be seen in Fig. 13, where we show Υ versus $\log T$ from Mohan et al. (1987) and the IRON Project, Υ rises only slightly at temperatures above

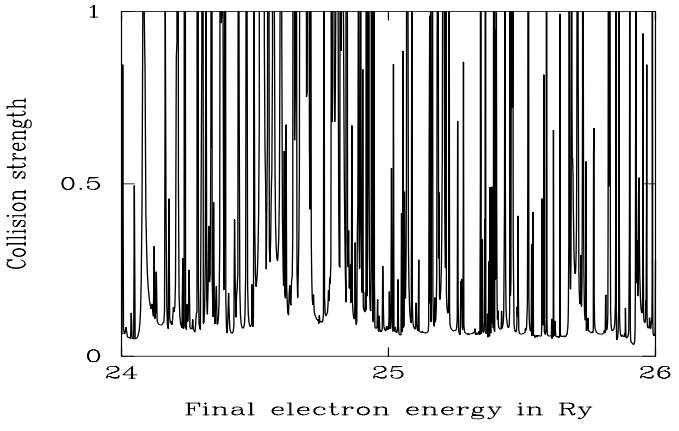

Fig. 7. Ca^{+11}: $\Omega(2p^5\ ^2P^o_{3/2},\ 2p^5\ ^2P^o_{1/2})$

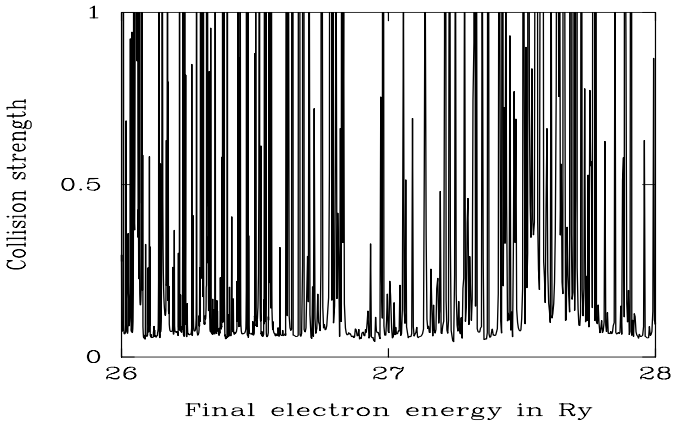

Fig. 8. Ca^{+11}: $\Omega(2p^5\ ^2P^o_{3/2},\ 2p^5\ ^2P^o_{1/2})$

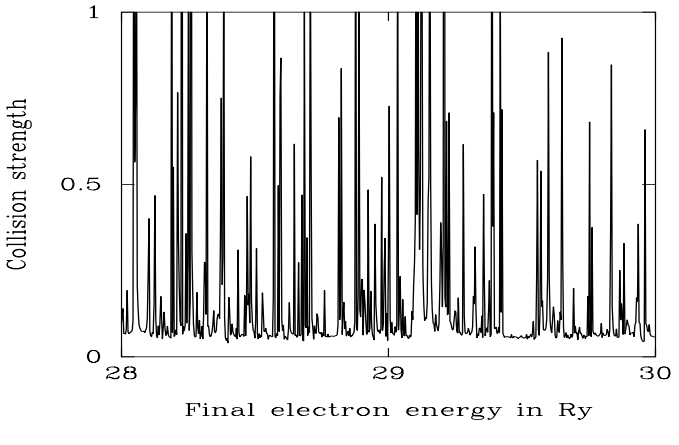

Fig. 9. Ca^{+11}: $\Omega(2p^5\ ^2P^o_{3/2},\ 2p^5\ ^2P^o_{1/2})$

Table 5. Fluorine sequence: thermally averaged collision strength $\Upsilon(2p^5\,P^o_{3/2}\,,\,2p^5\,P^o_{1/2}\,)$ as a function of the atomic number Z and the logarithm of the scaled temperature $T_s = T/(Z-8)^2$

$\log T_s$	$Z=12$	$Z=13$	$Z=14$	$Z=15$	$Z=16$	$Z=17$
3.0	3.579^{-1}	5.136^{-1}	3.014^{-1}	2.570^{-1}	2.408^{-1}	2.691^{-1}
3.2	3.605^{-1}	4.895^{-1}	3.793^{-1}	2.600^{-1}	2.674^{-1}	2.859^{-1}
3.4	3.679^{-1}	4.703^{-1}	4.176^{-1}	2.751^{-1}	2.883^{-1}	2.881^{-1}
3.6	3.827^{-1}	4.637^{-1}	4.351^{-1}	2.923^{-1}	2.968^{-1}	2.799^{-1}
3.8	4.045^{-1}	4.636^{-1}	4.340^{-1}	3.045^{-1}	2.974^{-1}	2.725^{-1}
4.0	4.289^{-1}	4.625^{-1}	4.241^{-1}	3.147^{-1}	2.996^{-1}	2.734^{-1}
4.2	4.482^{-1}	4.549^{-1}	4.081^{-1}	3.193^{-1}	2.986^{-1}	2.721^{-1}
4.4	4.518^{-1}	4.328^{-1}	3.796^{-1}	3.071^{-1}	2.824^{-1}	2.552^{-1}
4.6	4.334^{-1}	3.937^{-1}	3.369^{-1}	2.764^{-1}	2.500^{-1}	2.233^{-1}
4.8	3.960^{-1}	3.444^{-1}	2.872^{-1}	2.362^{-1}	2.103^{-1}	1.855^{-1}
5.0	3.491^{-1}	2.941^{-1}	2.393^{-1}	1.967^{-1}	1.724^{-1}	1.503^{-1}

$\log T_s$	$Z=18$	$Z=19$	$Z=20$	$Z=21$	$Z=22$	$Z=23$
3.0	4.206^{-1}	1.418^{-1}	1.577^{-1}	1.852^{-1}	2.168^{-1}	1.000^{-1}
3.2	3.572^{-1}	1.602^{-1}	1.702^{-1}	1.800^{-1}	1.916^{-1}	1.107^{-1}
3.4	3.093^{-1}	1.723^{-1}	1.734^{-1}	1.698^{-1}	1.697^{-1}	1.143^{-1}
3.6	2.736^{-1}	1.779^{-1}	1.719^{-1}	1.609^{-1}	1.567^{-1}	1.183^{-1}
3.8	2.541^{-1}	1.866^{-1}	1.769^{-1}	1.630^{-1}	1.590^{-1}	1.312^{-1}
4.0	2.511^{-1}	2.010^{-1}	1.889^{-1}	1.737^{-1}	1.694^{-1}	1.475^{-1}
4.2	2.488^{-1}	2.082^{-1}	1.939^{-1}	1.779^{-1}	1.717^{-1}	1.531^{-1}
4.4	2.321^{-1}	1.976^{-1}	1.821^{-1}	1.664^{-1}	1.585^{-1}	1.426^{-1}
4.6	2.014^{-1}	1.724^{-1}	1.573^{-1}	1.431^{-1}	1.348^{-1}	1.215^{-1}
4.8	1.656^{-1}	1.420^{-1}	1.286^{-1}	1.165^{-1}	1.087^{-1}	9.786^{-2}
5.0	1.327^{-1}	1.138^{-1}	1.026^{-1}	9.273^{-2}	8.576^{-2}	7.700^{-2}

$\log T_s$	$Z=24$	$Z=25$	$Z=26$	$Z=27$	$Z=28$
3.0	1.004^{-1}	1.062^{-1}	1.091^{-1}	1.033^{-1}	9.624^{-2}
3.2	1.073^{-1}	1.083^{-1}	1.048^{-1}	9.679^{-2}	8.698^{-2}
3.4	1.081^{-1}	1.055^{-1}	9.811^{-2}	9.036^{-2}	8.019^{-2}
3.6	1.112^{-1}	1.080^{-1}	9.694^{-2}	9.112^{-2}	8.175^{-2}
3.8	1.235^{-1}	1.221^{-1}	1.055^{-1}	1.012^{-1}	9.280^{-2}
4.0	1.382^{-1}	1.380^{-1}	1.165^{-1}	1.123^{-1}	1.044^{-1}
4.2	1.419^{-1}	1.417^{-1}	1.187^{-1}	1.137^{-1}	1.064^{-1}
4.4	1.308^{-1}	1.299^{-1}	1.088^{-1}	1.034^{-1}	9.695^{-2}
4.6	1.105^{-1}	1.088^{-1}	9.165^{-2}	8.644^{-2}	8.103^{-2}
4.8	8.845^{-2}	8.638^{-2}	7.317^{-2}	6.862^{-2}	6.432^{-2}
5.0	6.920^{-2}	6.695^{-2}	5.715^{-2}	5.341^{-2}	5.004^{-2}

one million degrees. The effective collision strength from Mohan et al. (1987) lies about 10% lower than the present one. This may be due to the fact that they include less target terms in their close-coupling expansion and use a much coarser energy mesh than we do. In Figs. 14 and 15 we compare the collision strength by Mohan et al. (1987) from the QUB atomic databank with the present calculation.

3.3. Ni XX

Mohan et al. (1990) tabulate Υ for this ion as a function of T. The range covered is from $T = 10^4$ to $T = 10^7$. Now according to Arnaud & Rothenflug (1985) Ni XX has its maximum coronal abundance at about $T = 6.3\,10^6$, so the tabulation by Mohan et al. does not cover the temperature range of interest fully. Figure 16 shows Υ as a function of $\log T$. The starred points ($*$) correspond to data taken from Table 1 in Mohan et al. (1990), while the full line curve represents the present results. Both sets of results have a maximum at a temperature below $\log T = 5$.

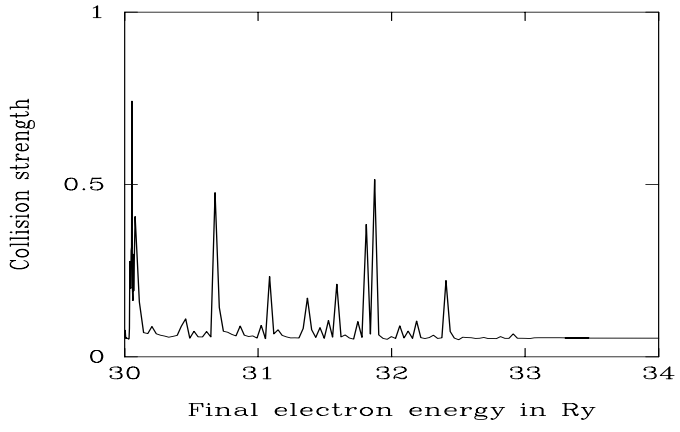

Fig. 10. Ca^{+11}: $\Omega(2p^5\ ^2P^o_{3/2},\ 2p^5\ ^2P^o_{1/2})$

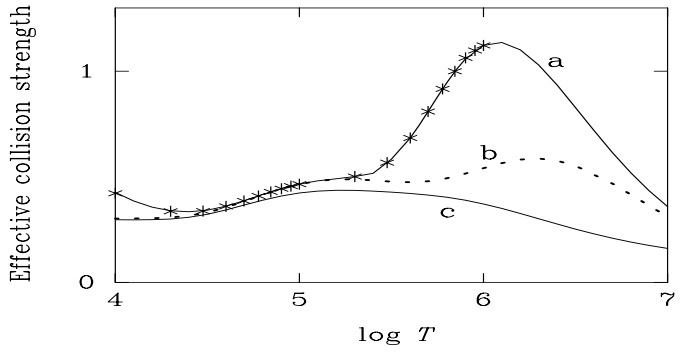

Fig. 11. Si^{+5}: Using Mohan & Le Dourneuf's (1990) Ω from the QUB atomic databank and **a)** the trapezoidal rule, **b)** the linear interpolation method. $*$: Mohan & Le Dourneuf (1990); **c)** IRON Project

Table 6. Showing how percentage contributions to Υ from four energy bands vary with temperature. The first 3 bands are identified by pairs of indices which label initial and final term energies. For example, the column headed 1, 2 is for integration from $E_f = \epsilon_1$ to $E_f = \epsilon_2$. Term energies are measured relative to the ground term, i.e. $\epsilon_1 = 0$. The last column is for the band that extends from ϵ_{28} to $E_f = \infty$. T_s is the scaled temperature defined by $T_s = T/(Z-8)^2$

Z	$\log T_s$	$1,2$	$2,3$	$3,28$	$28,\infty$
14	3.0	100	0	0	0
	4.0	85	14	1	0
	5.0	28	32	9	31
20	3.0	100	0	0	0
	4.0	48	50	1	1
	5.0	12	54	5	29
26	3.0	99	1	0	0
	4.0	31	67	1	1
	5.0	7	61	4	27

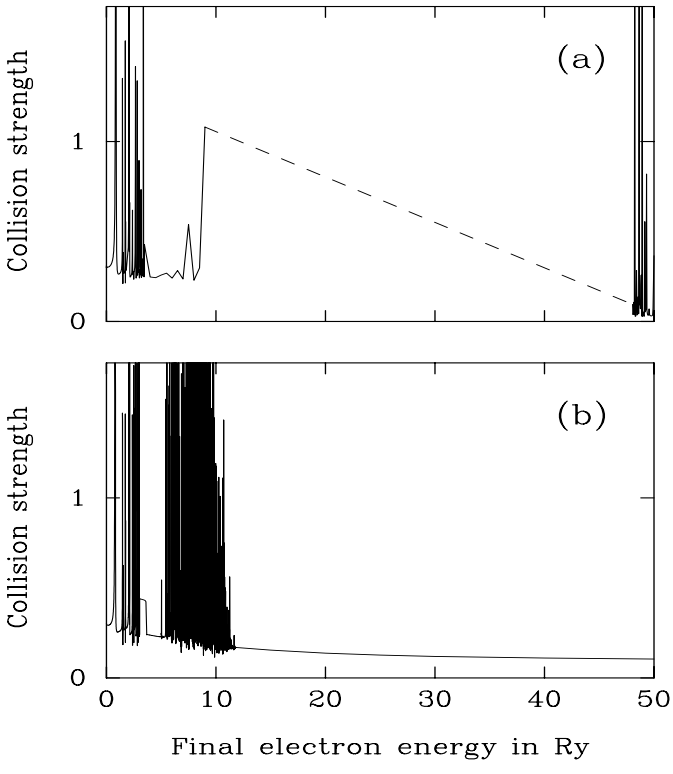

Fig. 12. Si^{+5}: **a)** Ω by Mohan & Le Dourneuf (1990) from the QUB atomic databank; **b)** IRON Project

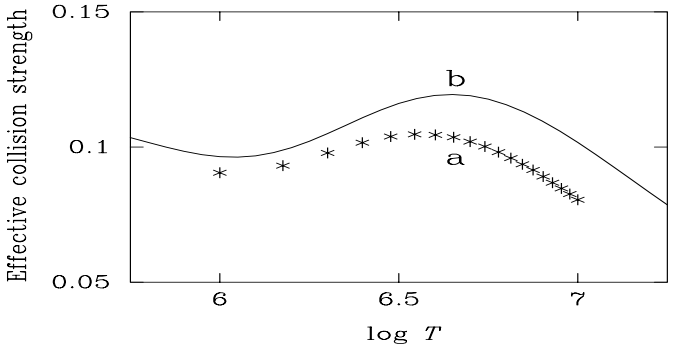

Fig. 13. Fe^{+17}: **a)** Mohan et al. (1987); **b)** IRON Project

Although the maxima occur at approximately the same value of $\log T$, they differ in size somewhat. At temperatures above 10^6, the present Υ exhibits a second peak which, although not present in the tabulation of Mohan et al. (1990), does show when we thermally average their collision strength from the QUB atomic databank. We conclude that Mohan et al. (1990) may have truncated the integration over energy too soon when calculating Υ.

4. Summary

The collision strength $\Omega(^2P^o_{3/2}, {}^2P^o_{1/2})$, for the ground term fine structure transition, is computed for fluorine like

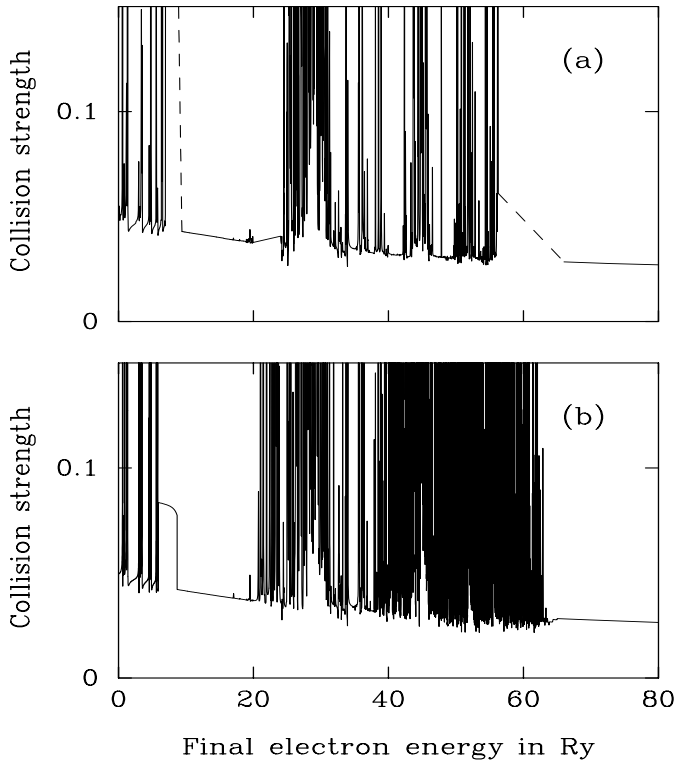

Fig. 14. Fe^{+17}: **a)** Ω by Mohan et al. (1987) from the QUB atomic databank; **b)** IRON Project

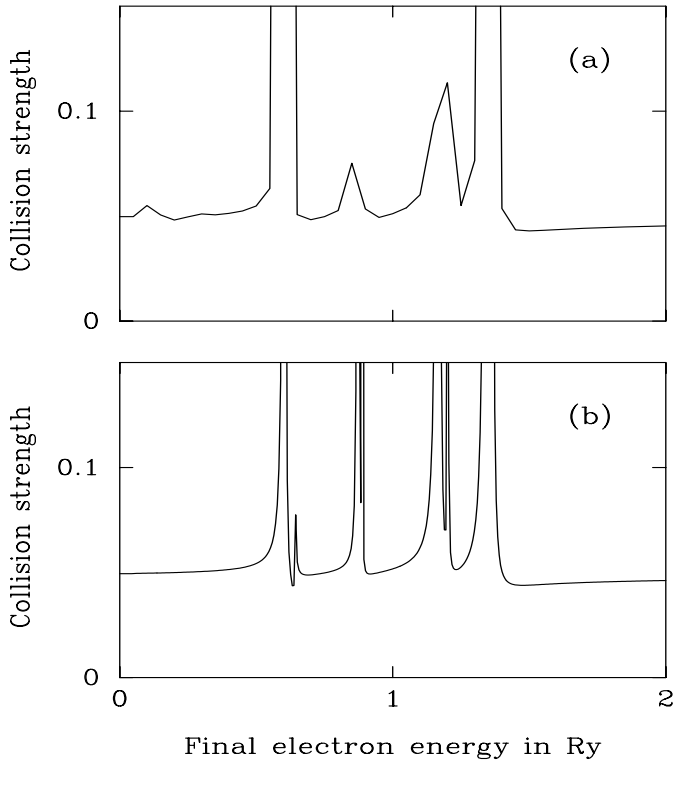

Fig. 15. Fe^{+17}: **a)** Ω by Mohan et al. (1987) from the QUB atomic databank; **b)** IRON Project

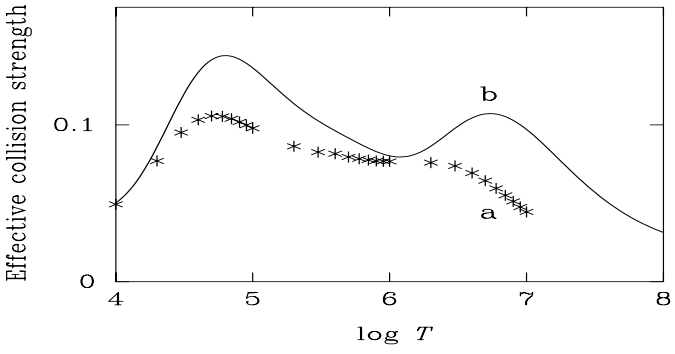

Fig. 16. Ni^{+19}: **a)** Mohan et al. (1990); **b)** IRON Project

ions from Mg IV to Ni XX at a fine enough energy mesh for one to be able to integrate accurately the product of Ω times the Maxwell velocity distribution function. The energy range covered suffices to obtain *effective collision strengths* up to and above the temperatures of maximum ionic abundance as compiled by Arnaud & Rothenflug (1985). The excitation rate coefficient in $\mathrm{cm^3\,s^{-1}}$ is

$$q(^2\mathrm{P}^\mathrm{o}_{3/2} \rightarrow {}^2\mathrm{P}^\mathrm{o}_{1/2}) = \frac{8.6287\ 10^{-6}}{\omega(\mathrm{P}^\mathrm{o}_{3/2})T^{1/2}}\ \Upsilon\ \exp\left(\frac{-\epsilon_{\mathrm{fs}}}{kT}\right), \qquad (4)$$

where $\omega = 4$ is the statistical weight of the ground level and k is Boltzmann's constant with the value $6.3335\ 10^{-6}$ Ry $\mathrm{K^{-1}}$. Numerical values of the fine structure transition energy ϵ_{fs} are given in Col. (c) of Table 4 for all elements in the isoelectronic sequence as far as nickel. We obtained these values using Edlén's (1969) formulas which accurately fit the observed intervals for $Z \leq 20$ and should provide reliable estimates for ions with $Z \geq 21$.

A comparison with the work by Mohan and co-workers, whose level of approximation is similar to ours, has shown the existence of some major disagreements. But we have been able to pinpoint the reasons for these and show that our results are more reliable than theirs.

Acknowledgements. This work was supported by the PPARC grant GR/H93576, and the EC network contract ERB CHRX CT920013. All of the figures were drawn using the graphics package called TVB ("Tracer vite et bien") which the author, Georges Gonczi of Nice Observatory, kindly made available. We wish to thank Alan Burgess and Alberto Binelli of Cambridge University and Werner Eissner of Bochum University for their constructive comments on an earlier version of the paper.

References

Arnaud M., Rothenflug R., 1985, A&AS 60, 425
Bautista M.A., 1996, A&AS 119, 105 (Paper XVI)
Bautista M.A., 1997, A&AS 122, 167 (Paper XX)

Bautista M.A., Pradhan A.K., 1996, A&AS 115, 551 (Paper XIII)
Bautista M.A., Pradhan A.K., 1997, A&AS 126, 365 (Paper XXVI)
Berrington K.A., 1995, A&AS 109, 193 (Paper VIII)
Berrington K.A., Pelan J.C., 1995, A&AS 114, 367 (Paper XII)
Berrington K.A., Tully J.A., 1997, A&AS 126, 105 (Paper XXIV)
Blackford H.M., Hibbert A., 1994, At. Data Nuc. Data Tables 58, 101
Burgess A., Tully J.A., 1992, A&A 254, 436
Burgess A., Chidichimo M.C., Tully J.A., 1997a, A&AS 121, 187
Burgess A., Chidichimo M.C., Tully J.A., 1997b, J. Phys. B: At. Molec. Opt. Phys. 30, 3
Burgess A., Chidichimo M.C., Mason H.E., Tully J.A., 1991, IR line radiation: A program for interpolating atomic collision data. In: Jashek C., Andrillat Y. (eds.) Proc. Int. Coll. Montpellier, France, 16-19 Oct. 1990. The infrared spectral region of stars. Camb. Univ. Press, Cambridge
Butler K., Zeippen C.J., 1994, A&AS 108, 1 (Paper V)
Clementi E., Roetti C., 1974, At. Data Nuc. Data Tables, 14, 177
Edlén B., 1969, Sol. Phys. 9, 439
Galavís M.E., Mendoza C., Zeippen C.J., 1995, A&AS 111, 347 (Paper X)
Galavís M.E., Mendoza C., Zeippen C.J., 1997, A&AS 123, 159 (Paper XXII)
Hibbert A., 1975, Comput. Phys. Commun. 9, 141
Hummer D.G., Berrington K.A., Eissner W., et al., 1993, A&A 279, 298 (Paper I)
Kisielius R., Berrington K.A., Norrington P.H., 1996, A&AS 118, 157 (Paper XV)
Lennon D.J., Burke V.M., 1994, A&AS 103, 273 (Paper II)
Mohan M., Baluja K.L., Hibbert A., Berrington K.A., 1987, MNRAS 225, 377
Mohan M., Hibbert A., 1991, Phys. Scr. 44, 158
Mohan M., Le Dourneuf M., 1990, Phys. Rev. A 41, 2862
Mohan M., Le Dourneuf M., Hibbert A., Burke P.G., 1990, MNRAS 243, 372
Nahar S.N., 1995, A&A 293, 967 (Paper VII)
Nahar S.N., Pradhan A.K., 1996, A&AS 119, 509 (Paper XVII)
Pelan J., Berrington K.A., 1995, A&AS 110, 209 (Paper IX)
Pelan J., Berrington K.A., 1997, A&AS 122, 177 (Paper XXI)
Quinet P., Le Dourneuf M., Zeippen C.J., 1996, A&AS 120, 361 (Paper XIX)
Saraph H.E., 1978, Comp. Phys. Commun. 15, 247
Saraph H.E., Tully J.A., 1994, A&AS 107, 29 (Paper IV)
Saraph H.E., Storey P.J., 1996, A&AS 115, 151 (Paper XI)
Seaton M.J., 1953, Proc. Roy. Soc. A 218, 400
Storey P.J., Mason H.E., Saraph H.E., 1996, A&A 309, 677 (Paper XIV)
Zhang H.L., Graziani M., Pradhan A.K., 1994, A&A 283, 319 (Paper III)
Zhang H.L., Pradhan A.K., 1995, A&A 293, 953 (Paper VI)
Zhang H.L., 1996, A&AS 119, 523 (Paper XVIII)
Zhang H.L., Pradhan A.K., 1997, A&AS 123, 575 (Paper XXIII)
Zhang H.L., Pradhan A.K., 1997, A&AS 126, 373 (Paper XXVII)